Anais do 51º Congresso Brasileiro do Concreto
CBC2009
Outubro / 2009

ISBN

APPLICATION OF NONLINEAR FRACTURE MECHANICS TO THE ASSESSMENT OF ROTATIONAL CAPACITY IN REINFORCED CONCRETE BEAMS

Alberto Carpinteri, Mauro Corrado
Politecnico di Torino, Italy

Politecnico di Torino
Department of Structural Engineering and Geotechnics

Outline

- **Introduction**
- **Snap-back instability in structural engineering**
- **Cohesive Crack Model**
- **Overlapping Crack Model**
- **Numerical algorithm for RC beams in bending**
- **Size-scale effects on the rotational capacity**
- **Size-scale effects on the minimum flexural reinforcement**

Ductility in structural design

The development of ductility is a key parameter for the design of RC beams in bending

The rotational capacity is required in order to:

- **provide structural robustness;**
- **give warning of incipient collapse by the development of large deformation prior to collapse;**
- **allow the bending moment redistribution in statically indeterminate structures;**
- **enable major distortions and energy dissipation during earthquakes;**
- **withstand impact and cyclic load.**

Different nonlinear contributions are involved in the flexural mechanical behaviour of RC elements

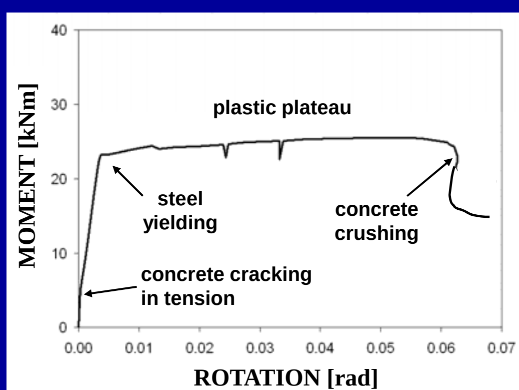

Traditional models, based on stress–strain constitutive laws for concrete and steel, do not capture the final softening branch, and define the ultimate condition by imposing limits to the materials deformations instead of by means of the drop of the resistant moment.

Evolution in the design formulae

1. The rotational capacity of RC beams in bending has been investigated from the experimental point of view in the early 1960s (CEB Indeterminate Structures Commission).

   The following empirical hyperbolic relationship between plastic rotation and relative neutral axis depth was proposed:

$$\vartheta_{PL} = \frac{0.004}{x/d}$$

Model Code 78

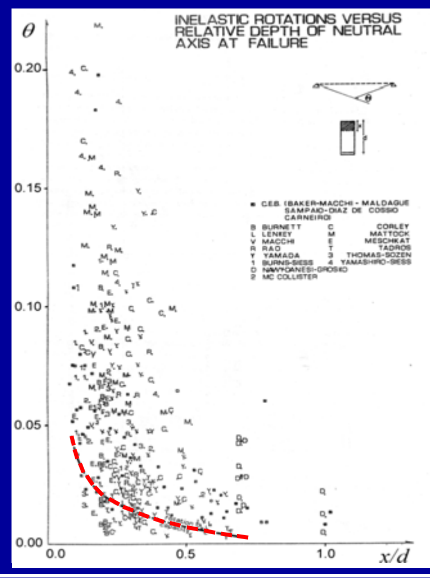

Siviero E. (1974) Rotation capacity of monodimensional members in structural concrete. *CEB Bull. Information*, **105**:206-222.

2. Analytical and experimental research coordinated by prof. Eligehausen

Two different collapse mechanisms (steel yielding and concrete crushing) and different steel ductility classes have been considered.

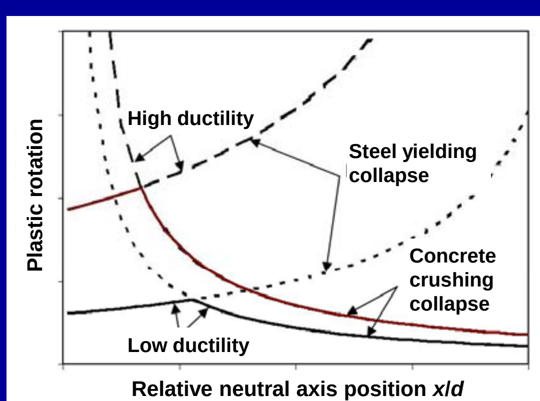

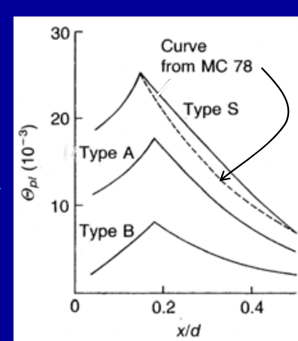

Model Code 90

Eligehausen R., Langer P. (1987) Rotation capacity of plastic hinges and allowable moment redistribution. *CEB Bull. Information*, **175**:17.9-17.29.

Eurocode 2

(EN 1992-1-1, 2004)

- When the plastic analysis is adopted in structural design, it has to verify that the admissible rotation in the plastic hinge is greater than the required rotation.

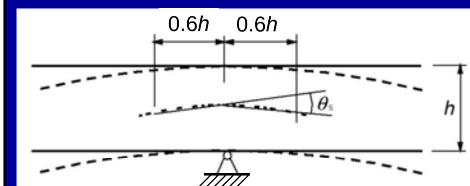

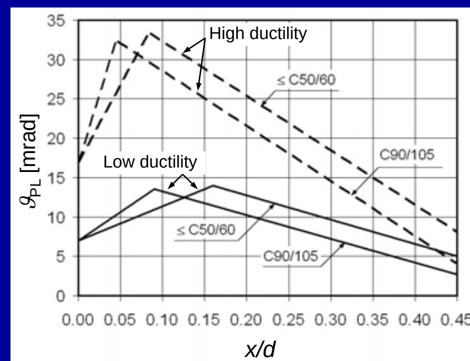

Experimental results

- **The ultimate rotation is a decreasing function of the structural size.**

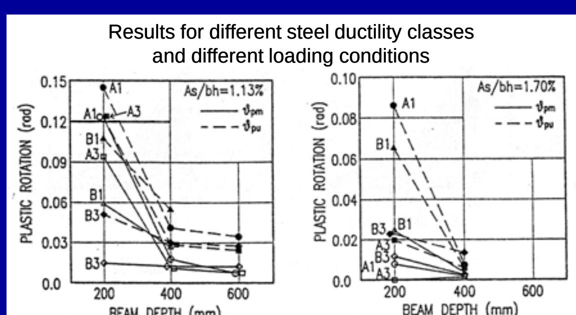

(Bosco and Debernardi 1993)

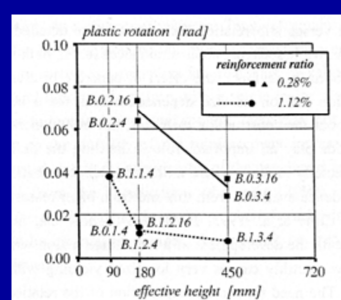

(Bigaj and Walraven 1993)

Corley G.W. (1966). Rotational capacity of reinforced concrete beams. *J. Struct. Division*, ASCE, **92**:121-146.

Mattock A.H. (1967). Rotational capacity of hinging regions in reinforced concrete beams. *Proc. Conf. on Flexural Mechanics of Reinf. Concrete*, SP-12, ACI/ASCE, 143-181.

Bosco C., Debernardi P.G. (1993). Influence of some basic parameters on the plastic rotation of reinforced concrete elements. *CEB Bull. Information*, **218**:25-44.

Bigaj A.J., Walraven J.C. (1993). Size effect on rotational capacity of plastic hinges in reinforced concrete beams. *CEB Bull. Information*, **218**:7-23.

Modelling the crack tip process zone in quasi-brittle and ductile materials

(a) CRACK TIP PROCESS ZONE

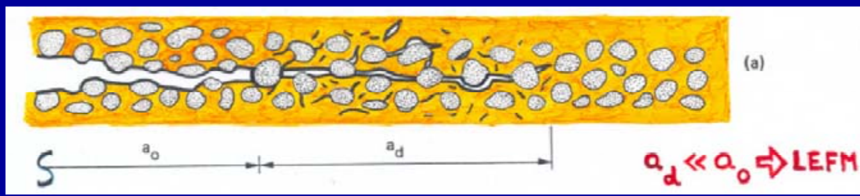

(b) COHESIVE FORCES behind the fictitious crack tip

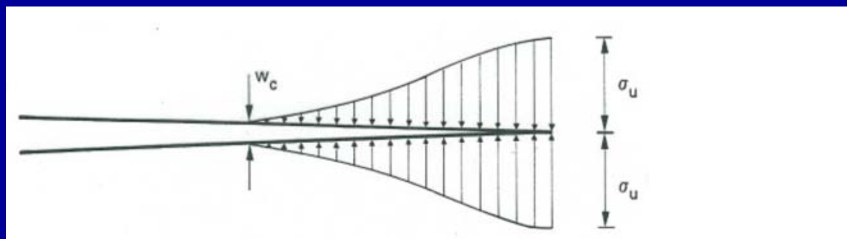

Development of Cohesive Zone Models

Dugdale (1960)	**crack-tip plastic zone (metals)**
Barenblatt (1962)	**cohesive atomic forces (crystals)**
Bilby, Cottrell & Swinden (1963)	**crack-tip plastic zone (metals)**
Rice (1968)	**crack-tip plastic zone (metals)**
Smith (1974)	**analysis of different cohesive laws (metals and concrete)**

Dugdale D.S. (1960) Yielding of steel sheets containing slits, *J. Mech. Phys. Solids* 8:100-114.

Barenblatt G.I. (1962) The mathematical theory of equilibrium cracks in brittle fracture, *Adv. App. Mech.* **7**:55-129.

Bilby B.A., Cottrell A.H., Swinden, K.H. (1963) The spread of plastic yield from a notch, *Proc. R. Soc. London* **A272**:304-314.

Rice J.R. (1968) A path independent integral and the approximate analysis of strain concentration by notches and cracks, *J. Appl. Mech.* **31**:379-386.

Smith E. (1974) The structure in the vicinity of a crack tip: a general theory based on the cohesive zone model, *Engng. Fract. Mech.* **6**:213-222.

Hillerborg et al. (1976)	**Fictitious Crack Model, for the analysis of Concrete (computational)**
Carpinteri (1984-1989)	**Cohesive Crack Model, for the analysis of snap-back instabilities (quasi-brittle mat's)**

Hillerborg A., Modeer M., Petersson P.E. (1976) Analysis of crack formation and crack growth in concrete by means of fracture mechanics and finite element. *Cem. Concr. Res.* **6**: 773-782.

Carpinteri A. (1985) Interpretation of the Griffith instability as a bifurcation of the global equilibrium. In: S.P. Shah (Ed.), *Application of Fracture Mechanics to Cementitious Composites* (Proc. of a NATO Adv. Res. Workshop, Evanston, USA, 1984), 284-316. Martinus Nijhoff Publishers, Dordrecht.

Carpinteri A. (1989) Cusp catastrophe interpretation of fracture instability, *J. Mech. Phys. Solids* **37**:567-582.

Carpinteri A. (1989) Decrease of apparent tensile and bending strength with specimen size: two different explanations based on fracture mechanics, *Int. J. Solids Struct*. **25**:407-429.

Carpinteri A. (1989) Post-peak and post-bifurcation analysis on cohesive crack propagation. *Engng. Fract. Mech.* **32**:265-278.

The problem of snap-back instability

Strain softening represents a violation of the Drucker's Postulate. As a consequence, the following phenomena may occur:

- **Loss of stability in the controlled load condition (*snap-through*);**
- **Loss of stability in the controlled displacement condition (*snap-back*).**

Maier G. (1966) Behaviour of elastic–plastic trusses with unstable bars, *ASCE J. Engng. Mech.*, **92**:67-91.

Maier G., Zavelani A., Dotreppe J.C. (1973) Equilibrium branching due to flexural softening, *ASCE J. Engng. Mech.*, **89**:897-901.

Carpinteri A. (1989) Softening and snap-back instability in cohesive solids, *Int. J. Num. Methods Engng.*, **28**:1521-1537.

Snap-back instabilities of the elastic equilibrium in thin shells

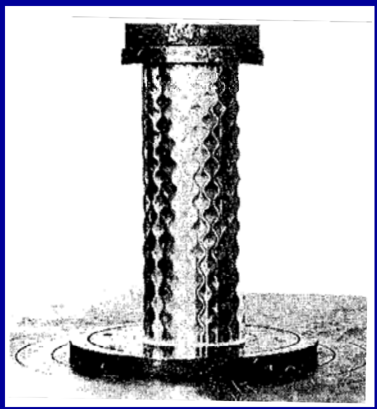

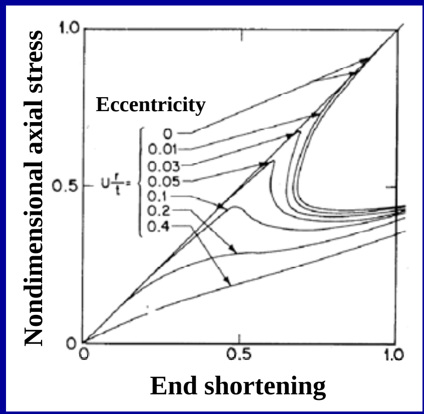

von Kármán T., Tsien H.S. (1941) The buckling of thin cylindrical shells under axial compression, *J. Aero. Sci.* **8**:303-312.

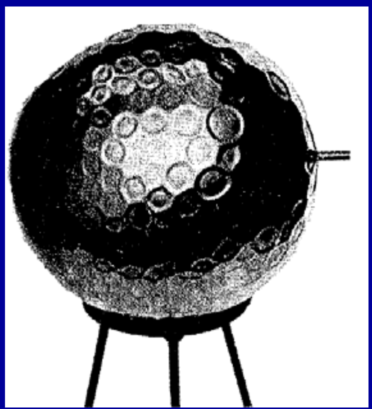

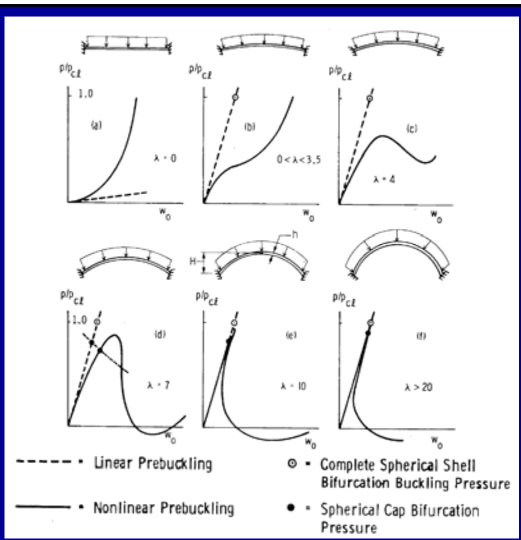

Carlson R.L., Sendlebeck R.L., Hoff N.J. (1967) Experimental studies of the buckling of complete spherical shells, *Exp. Mech.* **7**:281-288.

Kaplan A. (1974) Buckling of Spherical Shells, In: *Thin Shell Structures, Theory, Experiment, and Design*, Y.C. Fung and E.E. Sechler (eds.), Prentice-Hall, Inc., Englewood Cliffs, N.J., 248-288.

- **Case 1: *a* = 0**

  The load-deflection relation is linear: $\tilde{P} = \frac{4}{\lambda^3}\tilde{\delta}$ **, for** $\tilde{P} \leq 2/3 \ (\sigma \leq \sigma_u)$
- **Case 2: *a* = *h***

  The following equilibrium scheme can be considered:

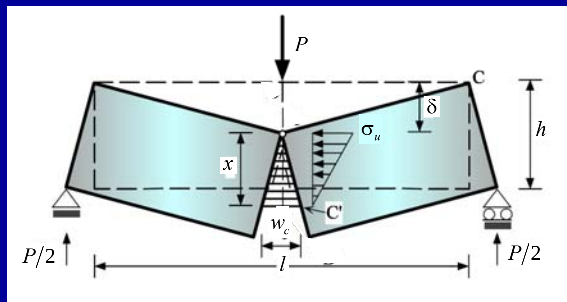

The load-deflection relation is hyperbolic ($s_E = \mathcal{G}_F / \sigma_u h$; $\lambda = l/h$):

$$\tilde{P} = \frac{1}{6}\left(\frac{s_E \lambda^2}{\varepsilon_u \tilde{\delta}}\right)^2, \text{ for } \tilde{P} \leq 2/3 \qquad (x \leq h)$$

Both equations have the same upper limit: $\tilde{P} \leq 2/3$ **.**

Carpinteri A. (1989) Size effects on strength, toughness, and ductility, *J. Eng. Mech.* **115**:1375-1392.

- **By transforming the load bounds into deflection bounds:**

$$\tilde{\delta} \leq \delta_1 = \frac{\lambda^3}{6} \quad \textbf{(1)} \qquad\qquad \tilde{\delta} \geq \delta_2 = \frac{s_E \lambda^2}{2\varepsilon_u} \quad \textbf{(2)}$$

a stability criterion for elastic-softening beams is obtained:

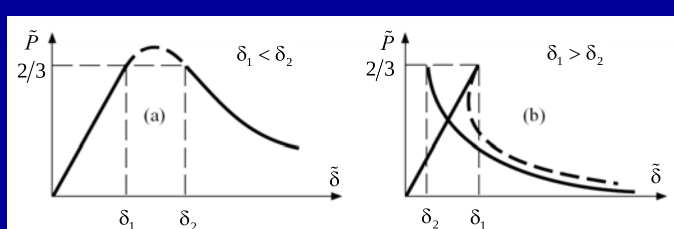

- **When the two domains are disjoint, the *P*–δ curve is regular;**
- **When they are partially overlapped, it is well-founded to suppose them connected by a curve with highly negative or even positive slope (snap-back).**
- **Snap-back is thus expected when $\delta_1 > \delta_2$** $\Rightarrow B = \frac{s_E}{\varepsilon_u \lambda} \leq \frac{1}{3}$ **.**

The Cohesive Crack Model

FRacture ANAlysis Code – ENEL-CRIS Milano and University of Bologna

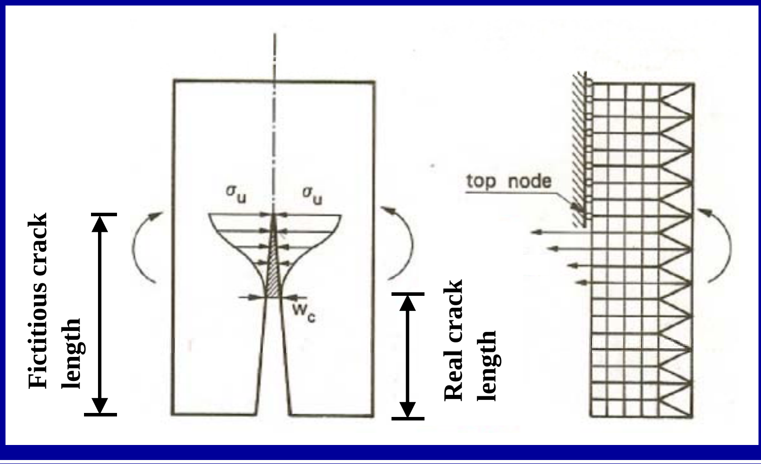

Carpinteri A. (1985) Interpretation of the Griffith instability as a bifurcation of the global equilibrium. In: S.P. Shah (Ed.), *Application of Fracture Mechanics to Cementitious Composites* (Proc. NATO Adv. Res. Workshop, Evanston, USA, 1984), 284-316. Martinus Nijhoff Publishers, Dordrecht.

Catastrophical behaviour

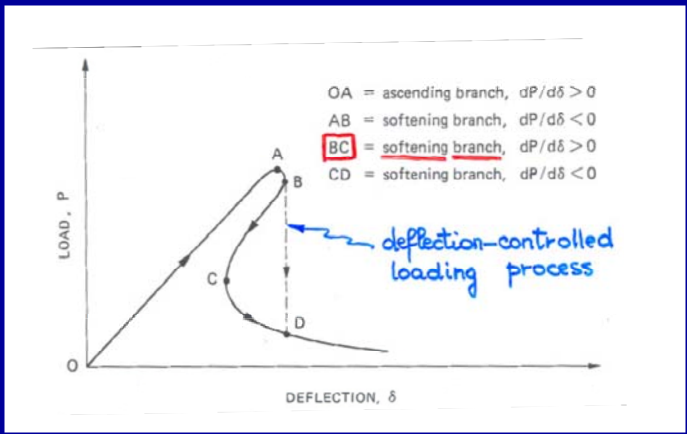

Carpinteri A. (1989) Cusp catastrophe interpretation of fracture instability, *J. Mech. Phys. Solids*, **37**:567-582.

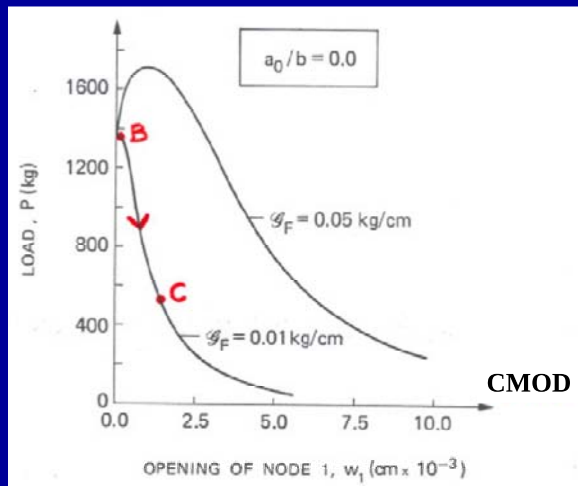

With a CMOD-controlled loading process, it is possible to follow the virtual softening branch BC.

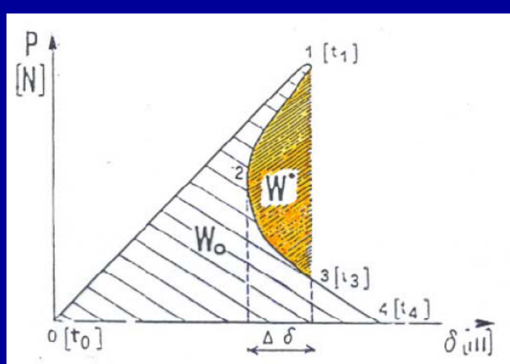

- The energy W* is released in the time period immediately following the achievement of the peak load.

- It can be measured dynamically through an impulse transducer.

Bocca P., Carpinteri A. (1990) Snap-back fracture instability in rock specimens: experimental detection through a negative impulse, *Engng. Fract. Mech.*, **35**:241-250.

Effect of the structural size-scale

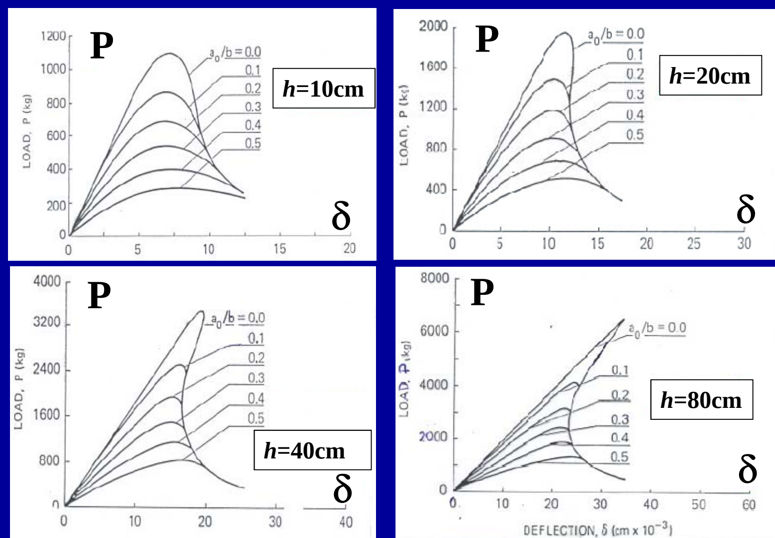

- **In the nondimensional $\tilde{P} - \tilde{\delta}$ plane, the mechanical behaviour is governed by the energy brittleness number, $s_E = \mathcal{G}_F / \sigma_u h$ (Carpinteri, 1985).**

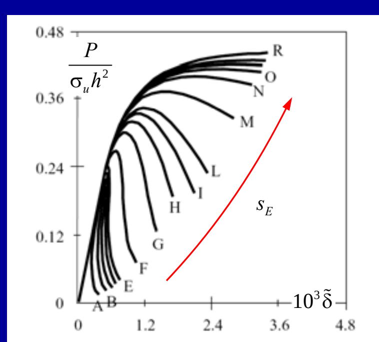

A:	$s_E = 2.09$	10^{-5}
B:	$s_E = 4.18$	10^{-5}
C:	$s_E = 6.27$	10^{-5}
D:	$s_E = 8.36$	10^{-5}
E:	$s_E = 10.45$	10^{-5}
F:	$s_E = 20.90$	10^{-5}
G:	$s_E = 41.80$	10^{-5}
H:	$s_E = 62.70$	10^{-5}
I:	$s_E = 83.59$	10^{-5}
L:	$s_E = 1.04$	10^{-3}
M:	$s_E = 2.08$	10^{-3}
N:	$s_E = 4.18$	10^{-3}
O:	$s_E = 6.27$	10^{-3}
P:	$s_E = 8.36$	10^{-3}
Q:	$s_E = 10.45$	10^{-3}
R:	$s_E = 20.90$	10^{-3}

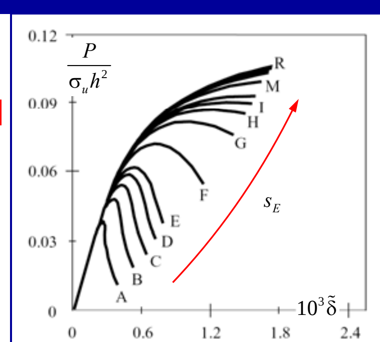

$a_0/h = 0$ $a_0/h = 0.5$

- **Snap-back condition:** $B \le \frac{1}{3} \Rightarrow s_E \le \frac{\varepsilon_u \lambda}{3} = 11.6 \times 10^{-5}$

$(\varepsilon_u = 0.87 \times 10^{-4};\ \lambda = 4)$

Size effects on tensile strength

- The ratio P_{Cohes}/P_{US} can be plotted against the nondimensional size, $1/s_E$.
- This ratio represents the ratio of the apparent tensile strength to the true tensile strength (considered as a material constant). It converges to unity for very small values of s_E.

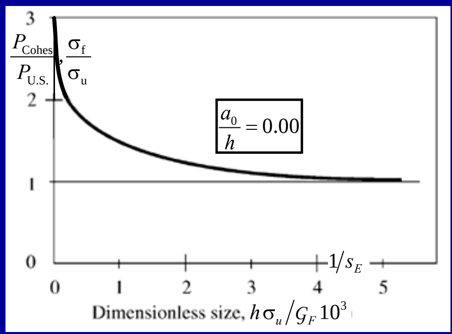

- The true tensile strength, σ_u, can be obtained only with very large specimens.

Comparison between Cohesive Crack Model and design codes

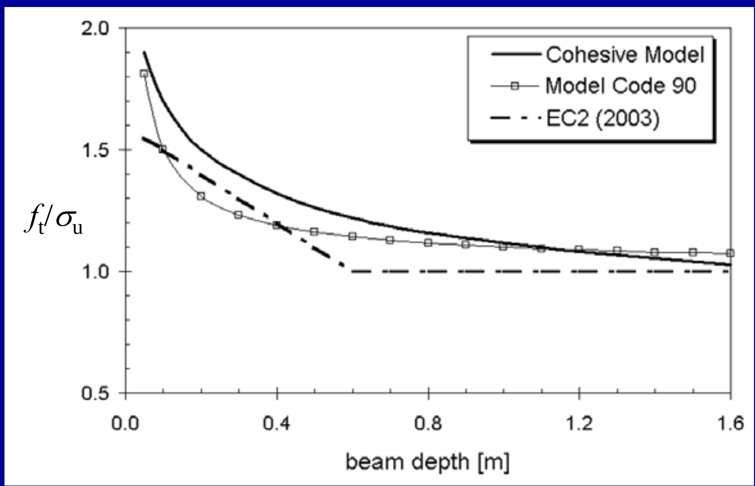

$\mathcal{G}_F$=0.1 kg/cm σ_u=20 kg/cm^2

The crucial role of the brittleness number

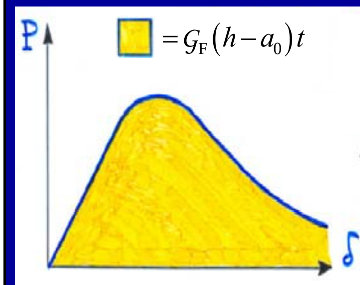

- **high fracture energy G_F**
- **low tensile strength σ_u**
- **small size *h***

$$s_E = \frac{\mathcal{G}_F}{\sigma_u h} \nearrow$$

large initial crack depth a_0/h
low slenderness *l/h*

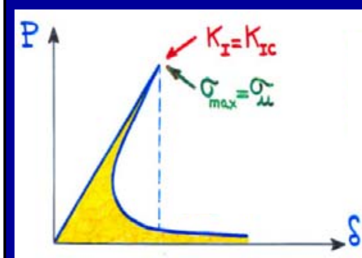

- **low fracture energy G_F**
- **high tensile strength σ_u**
- **large size *h***

$$s_E = \frac{\mathcal{G}_F}{\sigma_u h} \searrow$$

small initial crack depth a_0/h
high slenderness *l/h*

The Overlapping Crack Model

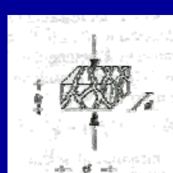

Crushing failure

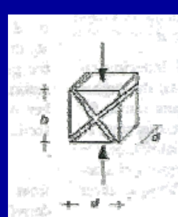

Shear failure

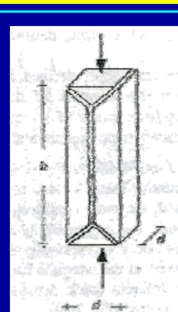

Splitting failure

Quasi-brittle materials show the phenomenon of strain localization also in compression when the elastic limit is overcome

Hudson J.A., Brown E.T., Fairhurst C. (1972) Shape of the complete stress-strain curve for rock. *Proc. of the 13th Symposium on Rock Mechanics*, Urbana, Illinois, 773-795.

van Mier J.G.M. (1984) *Strain softening of concrete under multiaxial compression*. PhD Thesis, Eindhoven.

Hillerborg A. (1990) Fracture mechanics concepts applied to moment capacity and rotational capacity of reinforced concrete beams. *Engng. Fract. Mech.*, **35**:233-240.

Jansen D.C., Shah S.P. (1997) Effect of length on compressive strain softening of concrete. *J. Eng. Mech.*, **123**:25-35.

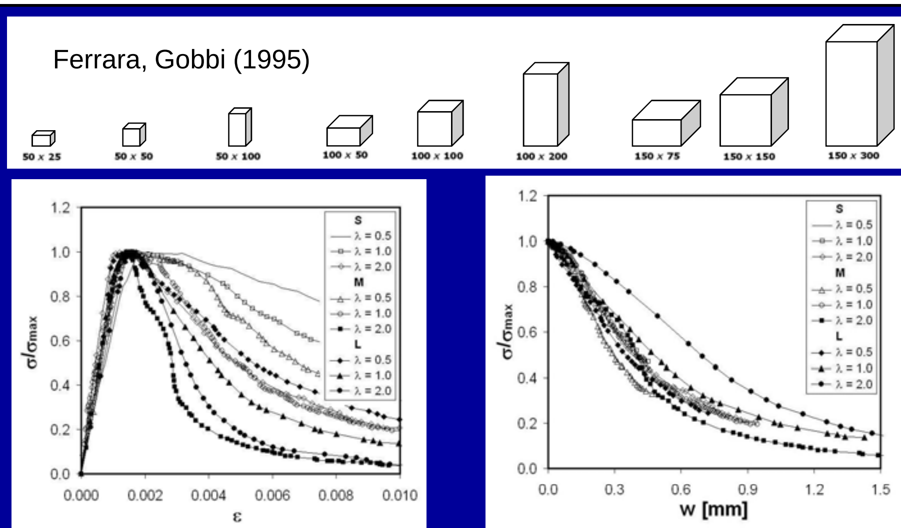

The slenderness- and scale-dependent curves collapse onto a narrow band!

Ferrara G., Gobbi M.E. (1995) Strain softening of concrete under compression. Report to RILEM Committee 148 SCC, Enel-CRIS Laboratory, Milano, Italy.

Evaluation of the post-peak overlapping, w

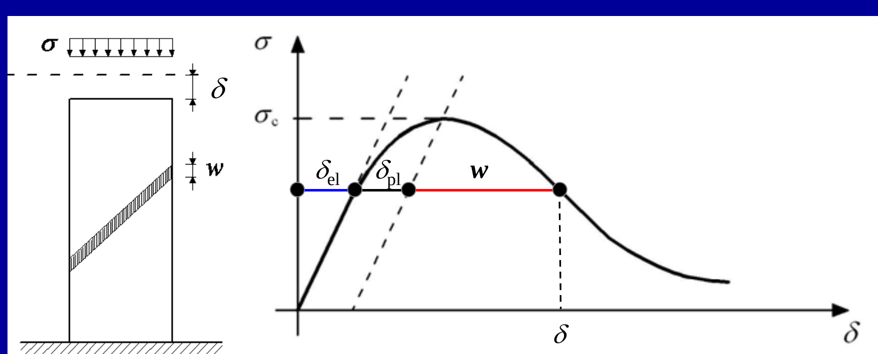

In analogy with the *Cohesive Crack Model*, the *Overlapping Crack Model* can be defined by a couple of constitutive laws:

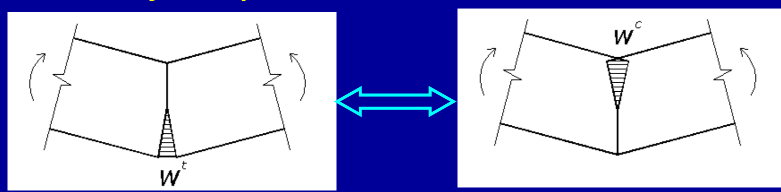

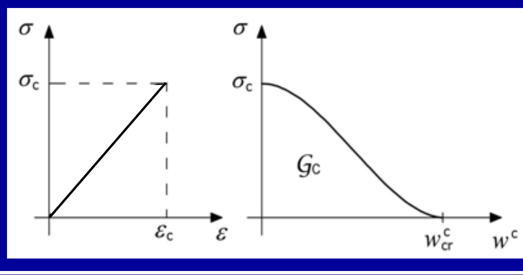

We define the *crushing* energy (per unit surface), as the area below the softening curve in the $\sigma - w$ diagram:

$$\mathcal{G}_C = 30 \div 60 \text{ N/mm}$$

$$w^c_{cr} \cong 1 \text{ mm}$$

Carpinteri A., Corrado M., Paggi M., Mancini G. (2007) Cohesive versus overlapping crack model for a size effect analysis of RC elements in bending, In: *Design, Assessment and Retrofitting of RC Structures*, Vol. 2 of FraMCoS-6, Taylor & Francis, 655-663.

Suzuki *et al.* (2006) Concentric loading test of RC columns with normal- and high-strength materials and average stress-strain model for confined concrete considering compressive fracture energy. *Proc. 2nd fib Congress*, Naples, Italy.

Application to uniaxial compression tests

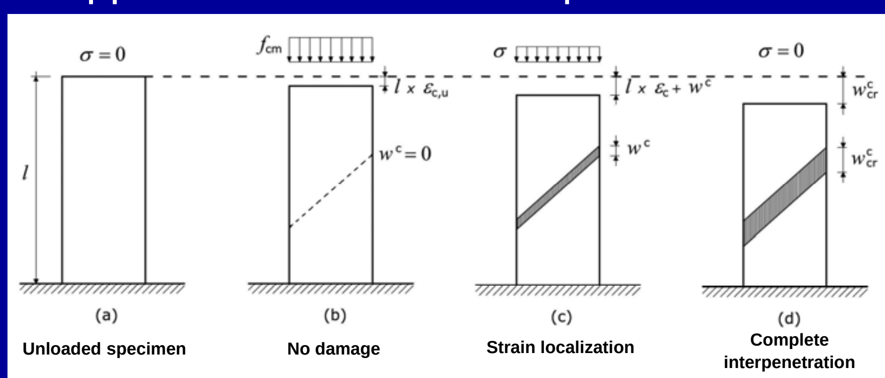

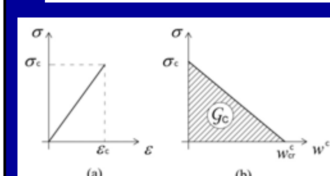

(b) $\delta = \dfrac{\sigma}{E} l,$ for $\varepsilon \leq \varepsilon_c$

(c) $\delta = \dfrac{\sigma}{E} l + w^c = \dfrac{\sigma}{E} l + w^c_{cr}\left(1 - \dfrac{\sigma}{\sigma_c}\right),$ for $w^c < w^c_{cr}$

(d) $\sigma = 0,$ for $w^c \geq w^c_{cr}$

Carpinteri A., Corrado M. (2009) An extended (fractal) Overlapping Crack Model to describe crushing size-scale effects in compression. *Eng. Failure Anal.*, **16**:2530-2540.

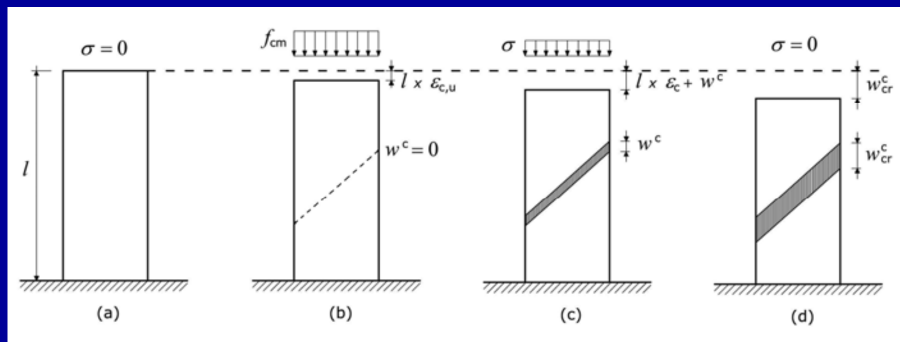

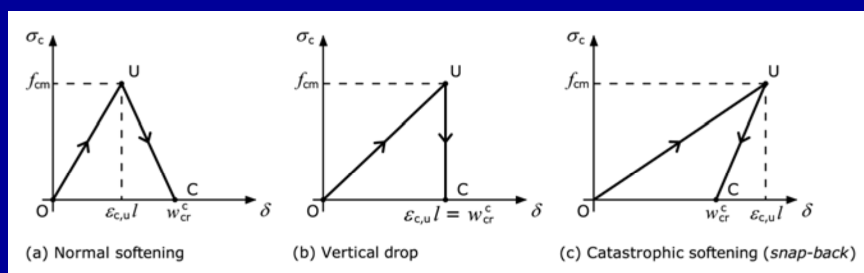

Experimental assessment: *normal strength concrete*

σ_c = 47.9 MPa

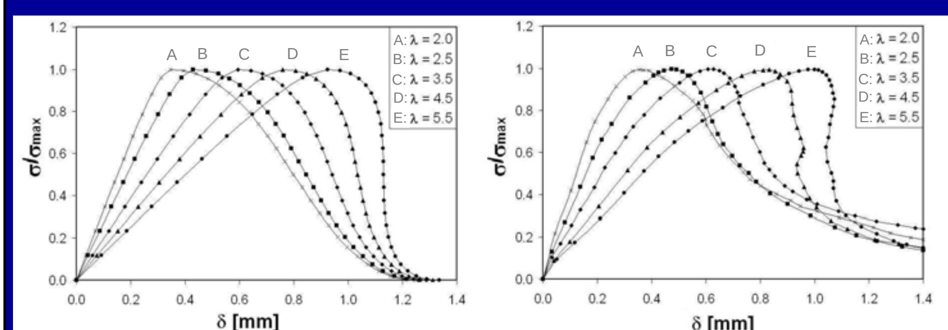

Numerical

Experimental

Jansen D.C., Shah S.P. (1997) Effect of length on compression strain softening of concrete. *J. Eng. Mech.*, **123**:25-35.

Carpinteri A., Corrado M., Mancini G., Paggi M. (2009) The overlapping crack model for uniaxial and eccentric concrete compression tests. *Mag. Concrete Res.*, **61**, in print.

Experimental assessment: ***high strength concrete***

$\sigma_c = 90.1\ \mathrm{MPa}$

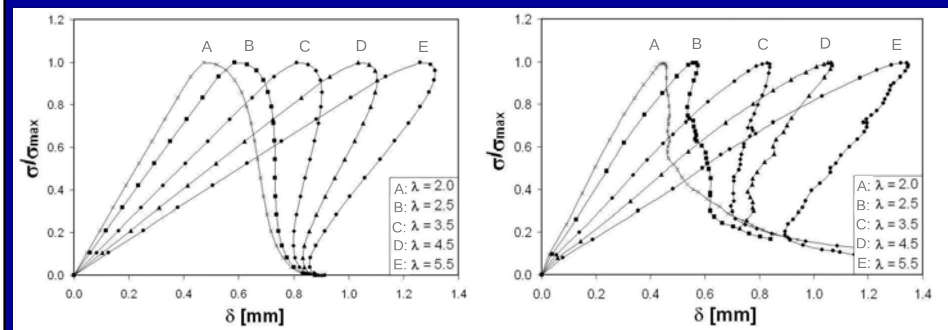

Numerical Experimental

Structural Ductility $\propto B = \dfrac{s_E^c}{\varepsilon_c \lambda} = \dfrac{\mathcal{G}_C}{h \sigma_c \varepsilon_c \lambda}$

Constitutive law for reinforcement

Bond-slip relationship (MC90)

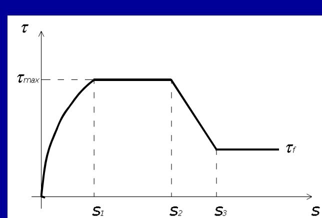

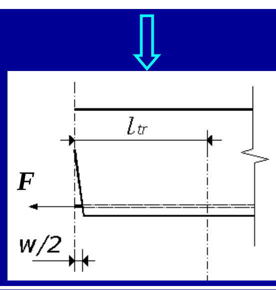

The reinforcement reaction and half the crack opening are given, respectively, by the integration of the bond stresses and the relative slips along the transfer length.

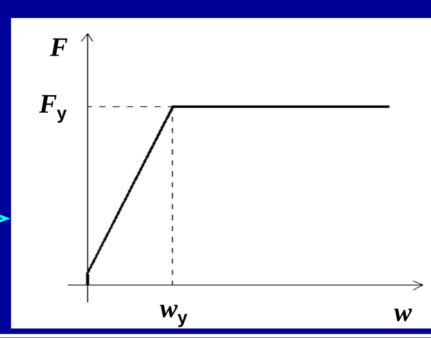

Ruiz G., Elices M., Planas J. (1999) Size effects and bond-slip dependence of lightly reinforced concrete beams. *Minimum reinforcement in concrete members*, A. Carpinteri, ed., Elsevier Science Ltd., Oxford, U.K., 127-180.

Numerical algorithm for RC beams in bending

Set consisting in *n* elastic equations:

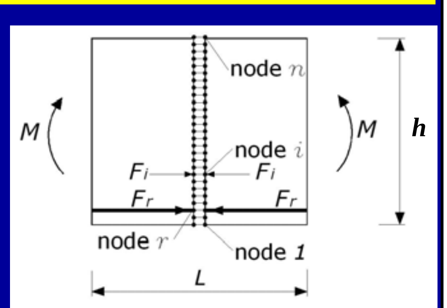

$$\{F\} = [K_w]\{w\} + \{K_M\}M$$

$\{F\}$ Nodal force vector

$[K_w]$ Influence coefficients matrix related to the nodal displacements (w_i = 1)

$\{w\}$ Opening/overlapping nodal displacements vector

$\{K_M\}$ Influence coefficients vector for the bending moment

M Applied bending moment

2*n*+1 unknowns: $\{F\}$, $\{w\}$ and M

Additional (*n*+1) equations:

$$F_i = 0 \quad \text{for} \quad i = 1, 2, \ldots, (j-1); \quad i \neq r$$

$$F_i = f(w_i) \quad i = r$$

$$F_i = F_u\left(1 - \frac{w_i^t}{w_{cr}^t}\right) \quad \text{for} \quad i = j, \ldots, (m-1)$$

$$w_i^t = 0 \quad \text{for} \quad i = m, \ldots, p$$

$$F_i = F_c\left(1 - \frac{w_i^c}{w_{cr}^c}\right) \quad \text{for} \quad i = (p+1), \ldots, n$$

***n* equations**

$F_m = F_u$ or $F_p = F_c$

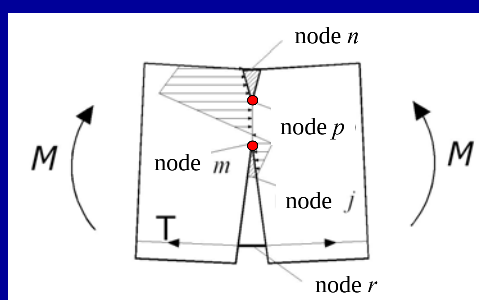

Governing parameter of the process

⇩

Position of the fictitious crack tip or the fictitious overlapping zone tip

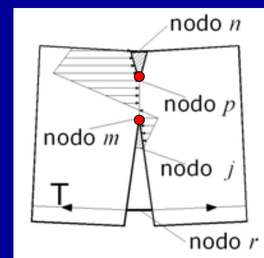

Computation of the rotation

At each step: $$\vartheta = \{D_w\}^T \{w\} + D_M M$$

$\{D_w\}$ vector of the coefficients of influence (nodal displacements)

$\{w\}$ vector of the nodal displacements (opening or overlapping)

D_M vector of the coefficients of influence (applied moment)

M applied moment

Experimental assessment of the proposed model

Bosco and Debernardi (1993)

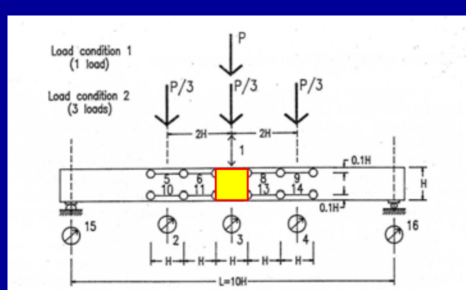

GEOMETRY

h = 200, 400, 600 mm
L/h= 10
ρ_t = 0.13% – 1.71%
ρ_c = 0.12% – 0.50%

CONCRETE

σ_u = 3 MPa
σ_c = 30 MPa
$\mathcal{G}_F$ = 0.065 N/mm
$\mathcal{G}_C$ = 30 N/mm

Bosco C., Debernardi P.G. (1993) Influence of some basic parameters on the plastic rotation of reinforced concrete elements. *CEB Bull. Information*, **218**:25-44.

Bending moment-rotation diagrams as functions of the beam size and of the reinforcement percentage

h = 200 mm

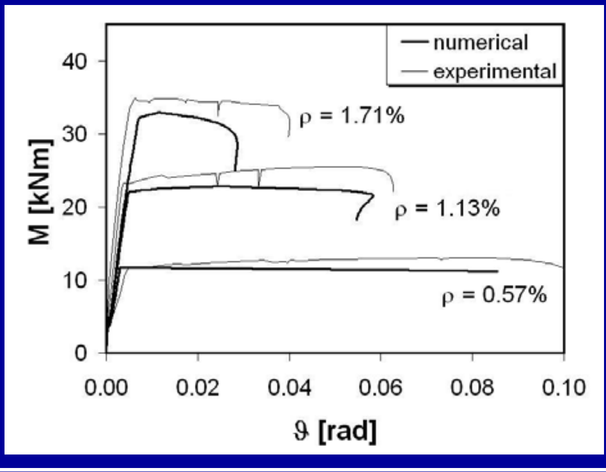

Carpinteri A., Corrado M., Mancini G., Paggi M. (2009) A numerical approach to modelling size effects on the flexural ductility of RC beams. *Mater. Struct.*, in print.

h = 400 mm

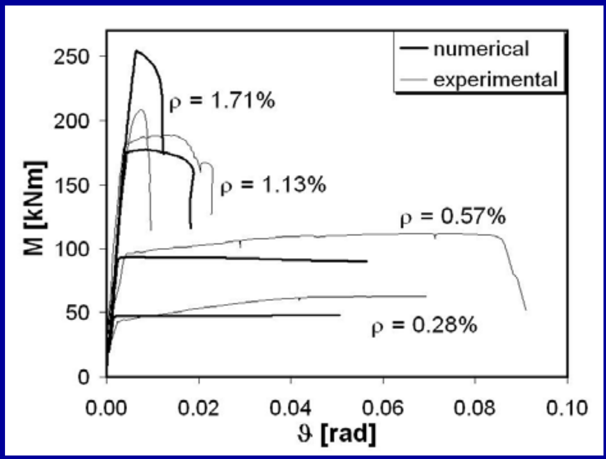

h = 600 mm

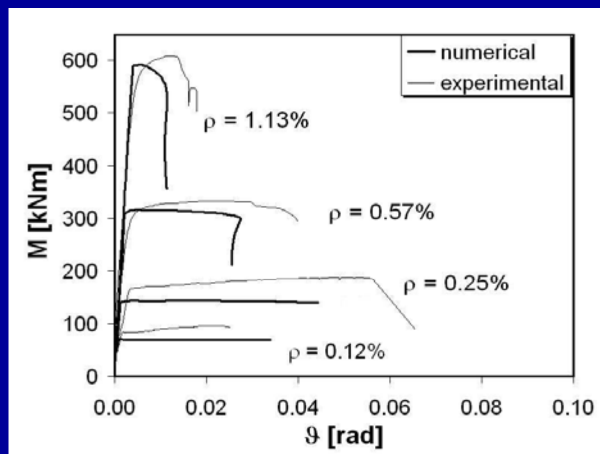

Size-scale effects on the rotational capacity

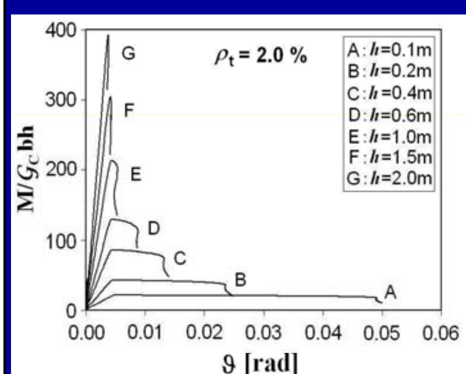

Numerical results

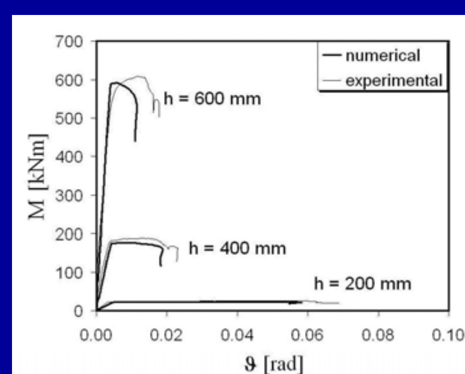

Numerical vs. experimental results, ρ_t = 1.13%

(Bosco and Debernardi 1993)

Effect of steel in compression

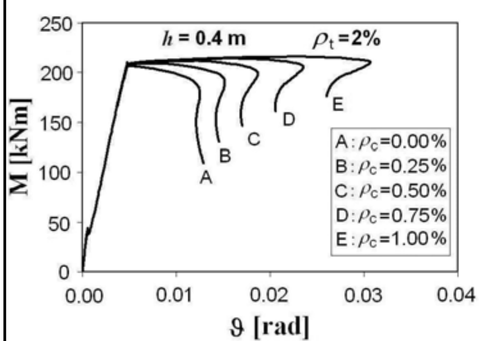

Moment vs. rotation response

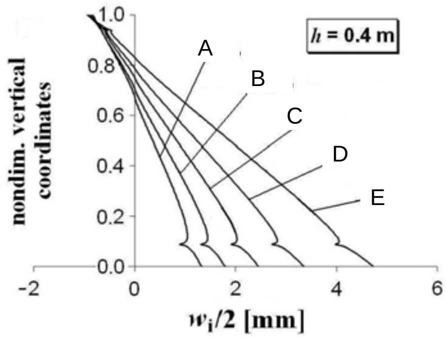

Horizontal nodal displacements at the maximum rotation

Effect of concrete compressive strength

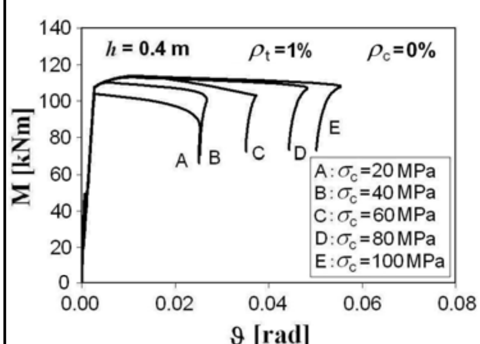

Moment vs. rotation response

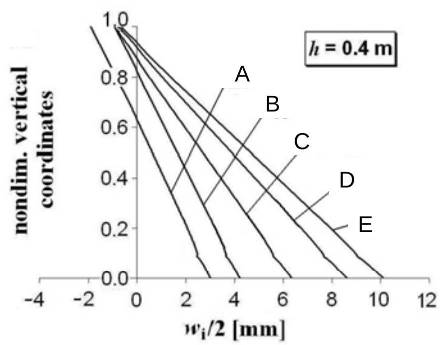

Horizontal nodal displacements at the maximum rotation

Effect of stirrups confinement

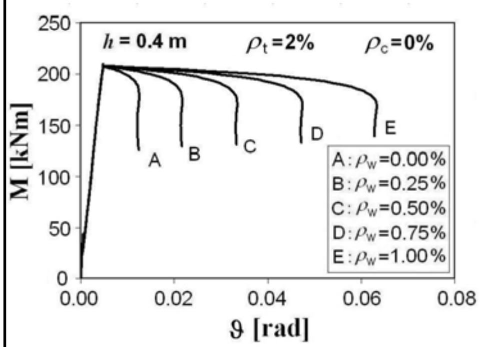

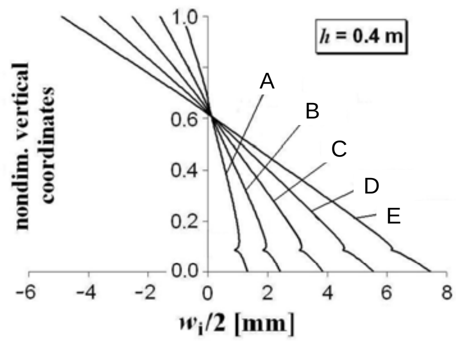

Moment vs. rotation response

Horizontal nodal displacements at the maximum rotation

Definition of plastic rotation

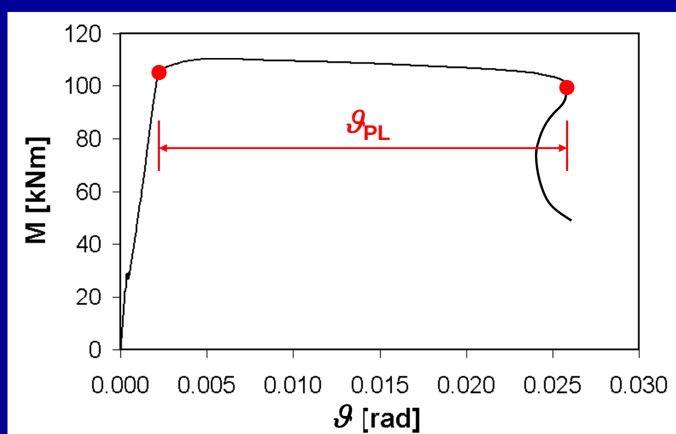

Comparison with the prescriptions of Eurocode 2

Eurocode 2: high ductility steel;
concrete compressive strength ≤ C50/60.

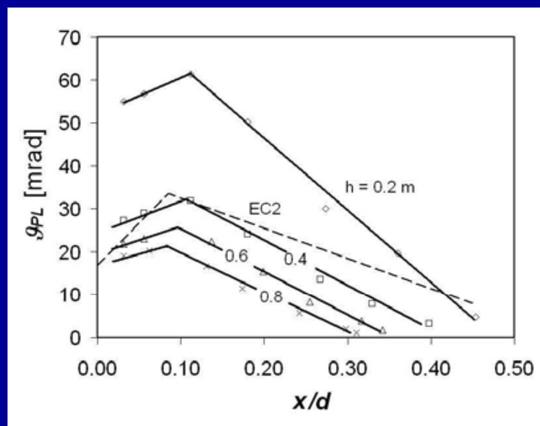

Carpinteri A., Corrado M., Mancini G., Paggi M. (2009) Size-scale effects on plastic rotational capacity of RC beams. *ACI Struct. J.*, **106** (6).

Size-scale effects on the minimum flexural reinforcement

Numerical vs. experimental results

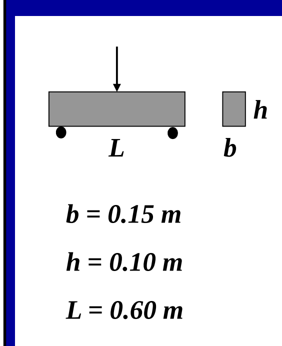

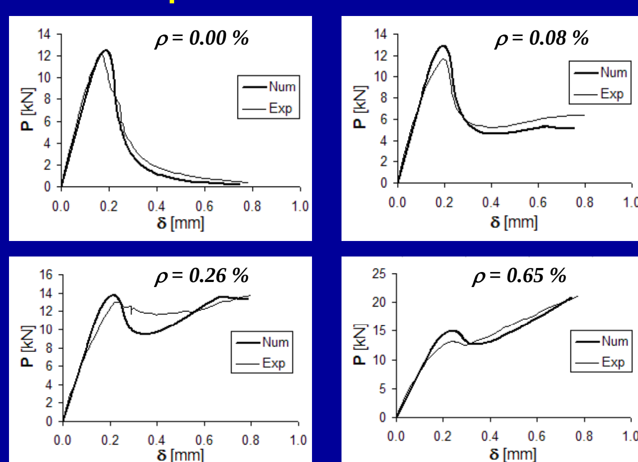

Bosco C., Carpinteri A., Debernardi P.G. (1990) Minimum reinforcement in high-strength concrete. *J. Struct. Eng.*, **116**:427-437.

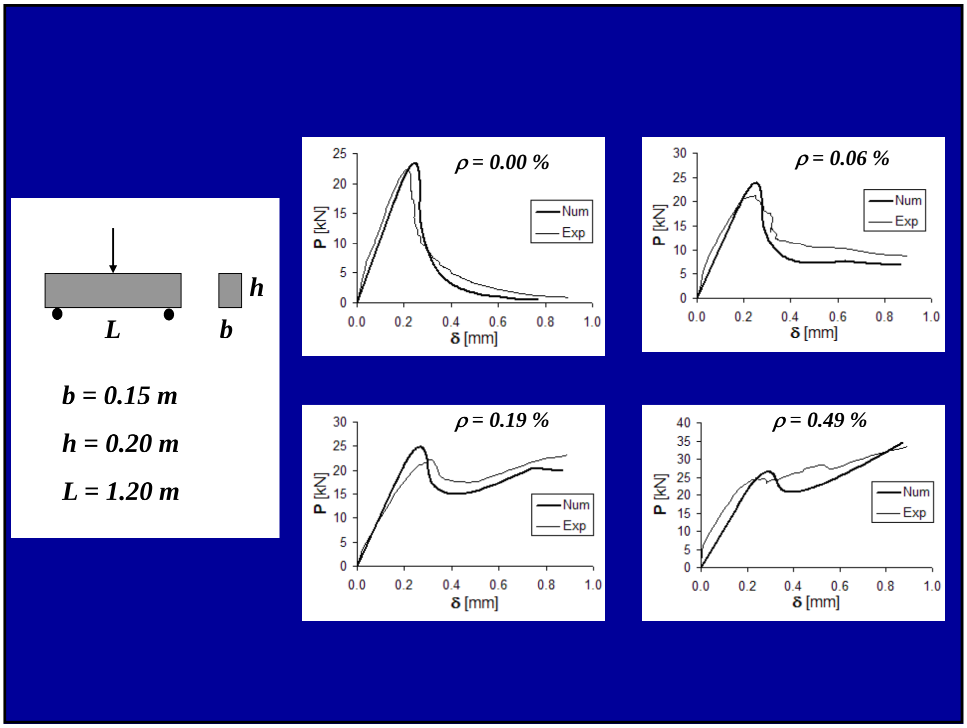
h
L
b
b = 0.15 m
h = 0.20 m
L = 1.20 m
ρ = 0.00 %
ρ = 0.06 %
ρ = 0.19 %
ρ = 0.49 %
P [kN]
δ [mm]
Num
Exp

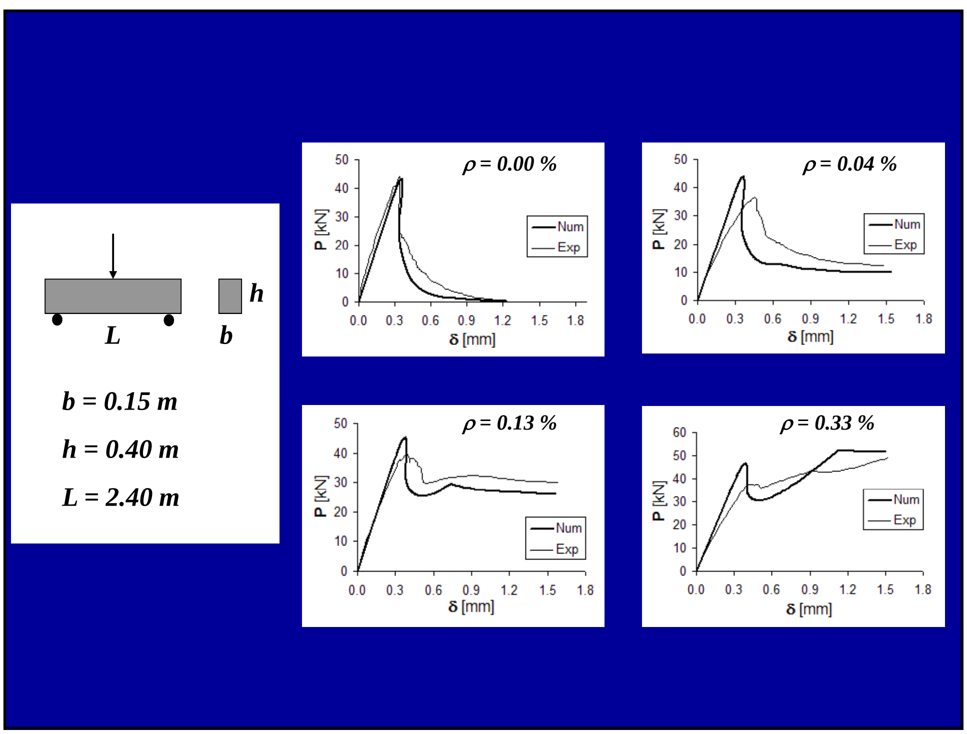
h
L
b
b = 0.15 m
h = 0.40 m
L = 2.40 m
ρ = 0.00 %
ρ = 0.04 %
ρ = 0.13 %
ρ = 0.33 %
P [kN]
δ [mm]
Num
Exp

Definition of minimum reinforcement

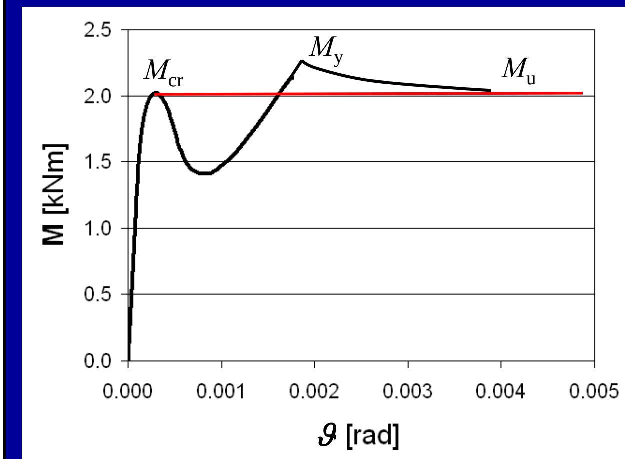

The global response is governed by two nondimensional numbers:

$$N_P = \rho \frac{\sigma_y h^{0.5}}{K_{IC}}$$

$$s = \frac{K_{IC}}{\sigma_u h^{0.5}}$$

being: $K_{IC} = \sqrt{\mathcal{G}_F E_c}$

In particular: $M_{cr} \propto \frac{1}{s}$ and $M_u \propto N_P$

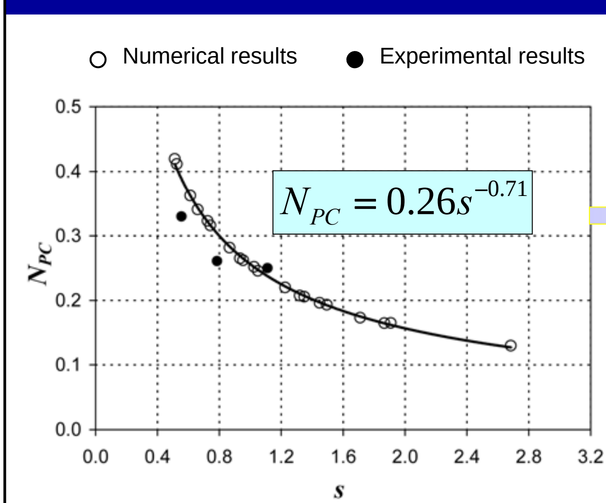

$$N_{PC} = \rho_{min} \frac{\sigma_y h^{0.5}}{K_{IC}}$$

$$\rho_{min} = 0.26 \frac{\sigma_u^{0.71} K_{IC}^{0.29}}{\sigma_y h^{0.15}}$$

Carpinteri A., Cadamuro E., Corrado M. Dimensional analysis approach to the assessment of the minimum flexural reinforcement in RC beams. To appear.

Comparison between different models

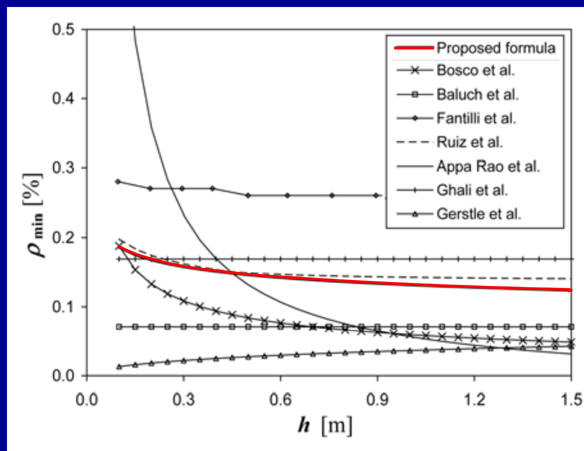

Comparison with Design Code formulae

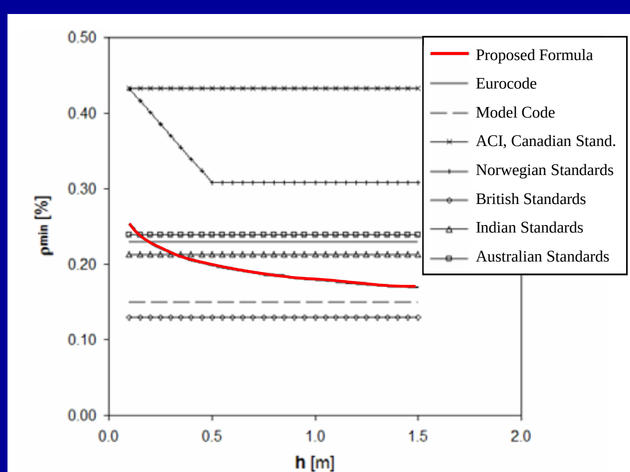

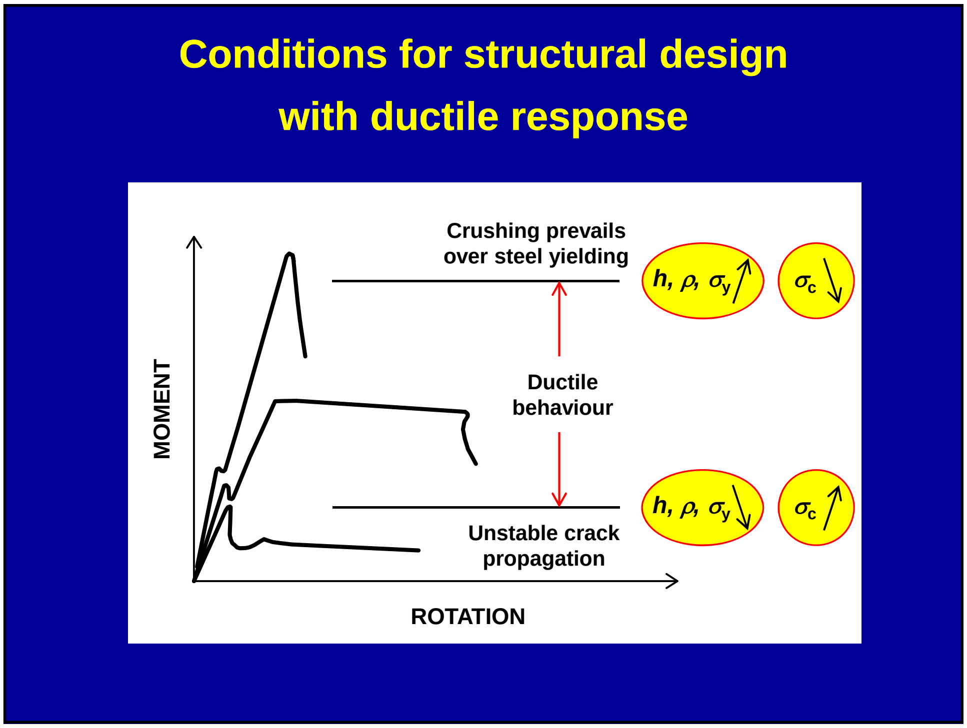
Conditions for structural design
with ductile response
Crushing prevails
over steel yielding
h, ρ, σy
σc
Ductile
behaviour
MOMENT
h, ρ, σy
σc
Unstable crack
propagation
ROTATION